Carrier to Interference Ratio Analysis for the Shotgun Cellular System

Prasanna Madhusudhanan*, Juan G. Restrepo†, Youjian (Eugene) Liu*, and Timothy X Brown*
* Department of Electrical and Computer Engineering, † Department of Applied Mathematics
University of Colorado, Boulder, CO 80309-0425 USA
Email: prasanna.madhusudhanan@colorado.edu, juanga@colorado.edu, eugeneliu@ieee.org, timxb@colorado.edu

***Abstract*—This paper analyzes the carrier-to-interference ratio of the so-called shotgun cellular system (SCS). In the SCS, base-stations are placed randomly according to a two-dimensional Poisson point process. Such a system can model a dense cellular or wireless data network deployment, where the base station locations end up being close to random due to constraints other than optimal coverage. The SCS is a simple cellular system where we can introduce several variations and design scenarios such as shadow fading, power control features, and multiple channel reuse groups, and assess their impact on the performance. We first derive an analytical expression for the characteristic function of the inverse of the carrier-to-interference ratio. Using this result, we show that the carrier-to-interference ratio is independent of the base station density and further, we derive a semi-analytical expression for the tail-probability. These results enable a complete characterization of the cellular performance of the SCS. Next, we incorporate shadow fading into the SCS and demonstrate that it merely scales the base station density by a constant. Hence, the cellular performance of the SCS is independent of shadow fading. These results are further used to analyze dense cellular scenarios.**

***Index Terms*—Cellular Radio, Co-channel Interference, Fading channels.**

I. Introduction

A shotgun cellular system (SCS) [1], [2] models minimally planned cellular systems by considering random placement of base-stations (BS) in the given region. In this model, the BSs are placed randomly over the entire plane according to a two-dimensional (2-D) Poisson point process with a parameter λ, which is the average BS density for the SCS. The density λ is assumed to be large enough that the BSs can provide wireless coverage for a mobile-station (MS) anywhere in the cellular system. This enables us to focus on the interference-limited cellular systems, and hence, we analyze the performance of the SCS by taking the carrier-to-interference ratio, $\frac{C}{I}$, as the performance metric. Further, we focus on the downlink (BS to MS) $\frac{C}{I}$ performance.

The SCS can represent many types of practical deployments. Dense cellular deployments mix cells of different sizes and end up with non-hexagonal cells. Uncoordinated deployments, such as wireless LANs as well as femtocells [3] which are cellsites placed by MS users in their homes, can appear random. Random radio placement has been considered in other wireless network analysis [4], [5]. Here we focus on analyzing SCS because they may provide a direct model for such practical deployments. Another motivation to study SCS arises from the fact that under shadow fading, the difference between ideal hexagonal system and the SCS has been shown to be small [2].

The SCS was analyzed in [2]. It was shown that the tail probability for the $\frac{C}{I}$ performance metric is given by $\text{Prob}\left(\left\{\frac{C}{I} > y \middle| y \geq 1, \varepsilon\right\}\right) = K_\varepsilon y^{-\frac{2}{\varepsilon}}$, where the constant $K_\varepsilon = \text{Prob}\left(\left\{\frac{C}{I} > 1 \middle| \varepsilon\right\}\right)$, and ε is the path loss exponent. Note that K_ε was determined via simulations and the behavior of the tail probability of $\frac{C}{I}$ in the region $0 \leq y < 1$ was not characterized. In Section III of this paper, an analytical expression for the characteristic function of $\left(\frac{C}{I}\right)^{-1}$ is derived. It is shown that the characteristic function of $\left(\frac{C}{I}\right)^{-1}$ is independent of λ, and hence, the distribution of $\frac{C}{I}$ is also independent of λ. A semi-analytical expression for the tail probability, $\text{Prob}\left(\left\{\frac{C}{I} > y \middle| \varepsilon\right\}\right)\ \forall\ y \in \mathbb{R}$, and hence, K_ε is obtained. Thus, the cellular performance of the SCS is characterized completely. In [2], it was conjectured, based on Monte-Carlo simulations, that the introduction of shadow fading to the SCS has no effect on the $\frac{C}{I}$-performance. In Section IV of this paper, it is shown analytically that when shadow fading is introduced to the SCS, the resulting system is equivalent to another SCS, with a different average BS density, $\bar{\lambda} = k\lambda$, where k is a constant which depends on the distribution of shadow fading. Since the shadow fading only scales the average BS density λ of the SCS, and the performance of the SCS is independent of λ, it is shown that the SCS is invariant to the shadow fading effects. This result is then extended in Section V to analyze power control in the SCS. Section VI incorporates multiple channel reuse groups (CG), Section VII briefly describes the simulation methods, and the conclusions can be found in Section VIII. Together these results strengthen the earlier results of [2] and provide additional insights to the SCS. The next section introduces the system model.

II. System Model

This section describes the various elements used to model the SCS (for more details, see [2], [6]). The BS layout, the radio environment and the performance metric constitute the elements of the SCS.

This work was supported in parts by NSF Grants CCF-0728955, ECCS-0725915.

978-1-4244-4148-8/09/$25.00 ©2009
This full text paper was peer reviewed at the direction of IEEE Communications Society subject matter experts for publication in the IEEE "GLOBECOM" 2009 proceedings.

A. BS Layout

In the SCS, BSs are placed according to a 2-D Poisson point process. A 2-D Poisson process is described by an average density parameter, λ. In such a setting, the probability that a BS exists in an infinitesimal area, dA, is given by λdA. It is assumed that λ is large enough that the BSs can provide coverage throughout the 2-D plane. It can be shown that, if R_1 is a random variable denoting the separation between the MS and the closest BS, then the probability density function (p.d.f.) of R_1 is given by $f_{R_1}(r_1) = \lambda 2\pi r_1 \mathrm{e}^{-\lambda\pi r_1^2}$, where $r_1 \geq 0$. Also, the conditional p.d.f. of the i^{th} closest BS conditioned on the $(i-1)^{\text{th}}$ closest BS, can be shown to be $f_{R_i|R_{i-1}}(r_i|r_{i-1}) = \lambda 2\pi r_i \mathrm{e}^{-\lambda\pi\left(r_i^2 - r_{i-1}^2\right)}$, where $r_i \geq r_{i-1}$. Such a model has previously been used to analyze ad-hoc packet radio networks [4], [5].

B. Radio Environment

In the SCS, all BSs are identical in terms of their transmission powers and antenna gains. Also, the BS and the MS antennas are assumed to be omni-directional. The signal from the BS to the MS undergoes path loss. The path loss follows an inverse power law, and is proportional to $R^{-\varepsilon}$, where ε is the path loss exponent, and R is the separation between the BS and the MS. It is assumed that $\varepsilon > 2$. Shadow fading captures the variations in the received signal power due to terrain, buildings and other obstructions that may lie between the BS and the MS. Overall, the received signal power at the MS in a cellular system, accounting for both the path-loss and the shadow fading, is given by $P = \frac{K\Psi}{R^{\varepsilon}}$, where K captures the transmission power of the BS and the antenna gains corresponding to the BS-MS pair, Ψ is the random shadow fading factor, and R is the separation between the BS and the MS. The shadow fading is often modeled by taking Ψ as a random number with a log-normal distribution [6], [7].

The SCS is considered to be an interference-limited cellular system, where the background noise and the thermal noise are negligible. As will be shown later, shadow fading effectively increases the density of a cellular system and further supports an intereference limited model of the system. In a cellular system with multiple CGs, adjacent CGs are assumed to be perfectly orthogonal to each other, and hence, the interference is only due to the co-channel interfering BSs.

C. Performance Metric

The performance measure that we are concerned about is the signal quality at the MS. The signal quality is defined as the ratio of the received signal power to the total interference power, and is denoted by $\frac{C}{I}$. For a given CG, the MS listens to the BS with the strongest received signal power P_S, where the subscript S stands for the signal-carrying BS. The interference is the sum of the received power from all the other co-channel BSs and is denoted by P_I. Without the shadow fading, the received signal power may be modeled as $P = KR^{-\varepsilon}$. In such systems, the BS closest to the MS is chosen as the signal-carrying BS in order to maximize $\frac{C}{I}$, and all other BSs are interfering BSs. When the shadow fading is introduced to such a system, the signal-carrying BS is not necessarily the BS closest to the MS. For a typical cellular system, the $\frac{C}{I}$ at the MS is given by $\frac{C}{I} = \frac{K_S \Psi_S R_S^{-\varepsilon}}{\sum_i K_i \Psi_i R_i^{-\varepsilon}}$, where K_S and $\{K_i\}$ capture the transmission power and antenna gains of the signal-carrying BS and the interfering BSs respectively; Ψ_S and $\{\Psi_i\}$ are the shadow fading factors corresponding to the signal-carrying BS and the interfering BSs respectively; R_S and $\{R_i\}$ are the separations between the corresponding BS-MS pairs.

For the SCS with no shadow fading or power control:

$$\frac{C}{I} = \frac{R_1^{-\varepsilon}}{\sum_{i>1} R_i^{-\varepsilon}}, \qquad (1)$$

since all the BSs in the system are identical, and the BS closest to the MS is the signal carrying BS. This case is analyzed in Section III. When shadow fading is introduced,

$$\frac{C}{I} = \frac{\Psi_S R_S^{-\varepsilon}}{\sum_i \Psi_i R_i^{-\varepsilon}}, \qquad (2)$$

where the subscript S is used to refer to the signal carrying BS, the subscript i is used to index the interfering BSs in the resulting system. This case is analyzed in Section IV. When power control features are introduced to the SCS,

$$\frac{C}{I} = \frac{K_S R_S^{-\varepsilon}}{\sum_i K_i R_i^{-\varepsilon}}, \qquad (3)$$

where, as before, the subscript S refers to the signal carrying BS, subscript i is used to index the interfering BSs. In the resulting system, each BS has a different transmission gain; K_S captures the transmission gain corresponding to the signal-carrying BS and $\{K_i\}$'s are the transmission gains corresponding to the interfering BSs. This system is analyzed in Section V.

III. Carrier to Interference Ratio of SCS

In this section, Theorem 1 is presented, where an analytical expression for the characteristic function of $\left(\frac{C}{I}\right)^{-1}$ is derived. Based on this theorem, a semi-analytical expression for the tail probability of $\frac{C}{I}$ is obtained. Using the tail probability, an expression for the constant K_ε (defined in Section I), is obtained.

Theorem 1: The characteristic function of $\left(\frac{C}{I}\right)^{-1}$ for the SCS is given by $\Phi_{\left(\frac{C}{I}\right)^{-1}}(\omega) = \frac{1}{{}_1F_1\left(-\frac{2}{\varepsilon}; 1-\frac{2}{\varepsilon}; i\omega\right)}$, where ${}_1F_1(\cdot;\cdot;\cdot)$ is the Confluent hypergeometric function. For the SCS with an average BS density λ, the distribution of $\frac{C}{I}$ is independent of λ.

Proof: In this proof, without loss of generality, the MS is assumed to be at the origin, and the system extends over the entire plane. First, the characteristic function of P_I (defined in Section II-C) is obtained for a given realization of R_1 (defined in Section II-A). Let r_1 denote one particular realization of R_1. The entire 2-D plane is divided into 2 regions; the first region being a circular area of radius r_1 centered at origin, and the second region is a ring from r_1 to r_B, where r_B will be taken to infinity later. The second region is further partitioned into $N-1$ concentric non-overlapping rings defined by the outer radius $r_j = r_1 + (j-1)\Delta r$, for $j = 2, 3, \cdots, N$. Each ring

978-1-4244-4148-8/09/$25.00 ©2009
This full text paper was peer reviewed at the direction of IEEE Communications Society subject matter experts for publication in the IEEE "GLOBECOM" 2009 proceedings.

has an incremental thickness $\Delta r = \frac{r_B - r_1}{N-1}$, and an incremental area $2\pi r_j \Delta r$. In each of these rings, a Bernoulli test is conducted to check whether there exists a BS or not, which, by the definition of the Poisson point process, happens with the probabilities $\lambda 2\pi r_j \Delta r + \mathrm{o}(\Delta r)$ and $1 - \lambda 2\pi r_j \Delta r + \mathrm{o}(\Delta r)$ respectively (the probability that there exists more than one BS in each ring is negligible since Δr is taken to be very small). The consequence of the Bernoulli test is mapped to a Bernoulli random variable X_j, which takes on values $K r_j^{-\varepsilon}$ and 0 respectively, to indicate the contribution to the interference at the MS from the j^{th} ring. Here, K is the quantity defined in Section II-B and is constant for all BSs in the SCS. By construction, $\{X_j\}$ is a set of independent random variables conditioned on a realization of R_1 (i.e. r_1). This is summarized as

$$\begin{aligned} \mathrm{Prob}\left(\{X_j = K r_j^{-\varepsilon}\}\right) &= \lambda 2\pi r_j \Delta r + o(\Delta r) \\ \mathrm{Prob}\left(\{X_j = 0\}\right) &= 1 - \lambda 2\pi r_j \Delta r + o(\Delta r), \quad (4) \end{aligned}$$

where $r_j > r_1$, and $P_I = \sum_{j=2}^{N} X_j$. Now, the characteristic function of X_j conditioned on R_1 can be written as

$$\begin{aligned} &\Phi_{X_j|R_1}(\omega \mid r_1) \\ &= 1 + \lambda 2\pi r_j \Delta r \left(\sum_{k=1}^{\infty} \frac{\left(i\omega K r_j^{-\varepsilon}\right)^k}{k!} \right) \quad (5) \\ &= \exp\left(\lambda 2\pi r_j \Delta r \left(\sum_{k=1}^{\infty} \frac{\left(i\omega K r_j^{-\varepsilon}\right)^k}{k!} \right) \right) + o(\Delta r), \quad (6) \end{aligned}$$

where the higher order powers of Δr are included, to obtain (6) from (5). Using (6), the characteristic function of P_I conditioned on R_1 is given by

$$\begin{aligned} &\Phi_{P_I|R_1}(\omega|r_1) \\ &\overset{(a)}{=} \lim_{r_B \to \infty} \lim_{N \to \infty} \prod_{j=2}^{N} \Phi_{X_j|R_1}(\omega|r_1) \\ &\overset{(b)}{=} \lim_{r_B \to \infty} \lim_{N \to \infty} \exp\left(\sum_{j=2}^{N} \lambda 2\pi r_j \Delta r \left(\sum_{k=1}^{\infty} \frac{\left(i\omega K r_j^{-\varepsilon}\right)^k}{k!} \right) \right) \\ &+ o(\Delta r) \\ &\overset{(c)}{=} \exp\left(\int_{r=r_1}^{\infty} \lambda 2\pi r \left(\sum_{k=1}^{\infty} \frac{\left(i\omega K r^{-\varepsilon}\right)^k}{k!} \right) dr \right) \\ &\overset{(d)}{=} \exp\left(\sum_{k=1}^{\infty} \left(\frac{(i\omega K)^k \lambda 2\pi}{k!} \int_{r=r_1}^{\infty} r^{1-k\varepsilon} dr \right) \right) \\ &\overset{(e)}{=} \exp\left(-\lambda\pi r_1^2 \left(-1 + \sum_{k=0}^{\infty} \frac{\left(i\omega K r_1^{-\varepsilon}\right)^k \times \left(-\frac{2}{\varepsilon}\right)_k}{k! \times \left(1 - \frac{2}{\varepsilon}\right)_k} \right) \right) \\ &\overset{(f)}{=} \exp\left(\lambda\pi r_1^2 \left(1 - {}_1F_1\left(-\frac{2}{\varepsilon}; 1 - \frac{2}{\varepsilon}; i\omega K r_1^{-\varepsilon} \right) \right) \right), \quad (7) \end{aligned}$$

where (a) follows from the definition on P_I; (b) follows from the fact that P_I is the sum of $\{X_j\}$ which are independent random variables, (c) transforms the infinitesimal summation to an integration over the entire range, (d) exchanges the orders of summation and integration (justified by the convergence of the integral due to the fact that $\varepsilon > 2$), (e) is obtained by rewriting the result of the integration in terms of Pochammer symbol $(a)_k$, defined as $(a)_k = a(a+1)\cdots(a+k-1)$, $(a)_0 = 1$, $a \neq 0$, and finally (f) is obtained by relating the summation in (g) to a Confluent hypergeometric function. A Confluent hypergeometric function is defined by ${}_1F_1(a;b;x) = \sum_{k=0}^{\infty} \frac{x^k (a)_k}{k! (b)_k}$.

Now, taking the expectation with respect to R_1 on $\Phi_{\left(\frac{P_I}{P_S}\right)|R_1}(\omega|r_1)$ gives the unconditioned characteristic function of $\left(\frac{C}{I}\right)^{-1} = \frac{P_I}{P_S}$. Note that $P_S = K R_1^{-\varepsilon}$ (see Section II-C) conditioned on R_1 is just a constant. Thus, the characteristic function of $\left(\frac{C}{I}\right)^{-1}$ is

$$\begin{aligned} &\Phi_{\left(\frac{C}{I}\right)^{-1}}(\omega) \\ &\overset{(a)}{=} \mathrm{E}_{R_1}\left(\Phi_{\left(\frac{P_I}{P_S}\right)|R_1}(\omega|r_1) \right) \\ &\overset{(b)}{=} \int_{r_1=0}^{\infty} \lambda 2\pi r_1 e^{-\lambda\pi r_1^2} e^{\left(\lambda\pi r_1^2\left(1 - {}_1F_1\left(-\frac{2}{\varepsilon}; 1 - \frac{2}{\varepsilon}; i\omega\right)\right)\right)} dr_1 \\ &\overset{(c)}{=} \frac{1}{{}_1F_1\left(-\frac{2}{\varepsilon}; 1 - \frac{2}{\varepsilon}; i\omega\right)}, \quad (8) \end{aligned}$$

where (a) follows from the definition of expectation, (b) is obtained by finding $\Phi_{\frac{P_I}{P_S}|R_1}(\omega|r_1)$ in terms of $\Phi_{P_I|R_1}(\omega|r_1)$ and expanding the expectation in the integral form, and (c) follows directly from the integration. From (8), it follows that the characteristic function of $\left(\frac{C}{I}\right)^{-1}$ is not a function of the BS density. Hence, the distribution of $\frac{C}{I}$ is also independent of λ. ■

Figure 1 shows the plot of the moments of $\left(\frac{C}{I}\right)^{-1}$ obtained from the characteristic function compared with those obtained by Monte-Carlo simulations (for details, see Section VII). It is clear that the simulation result approaches the true moment as the number of iterations are increased. Still, there is some gap even for iterations as high as 150000. Thus, having an analytical expression actually helps as enhanced accuracy is gained in addition to the fact that the need to perform simulations in order to derive information about the SCS performance is obviated.

Using the above characteristic function, an expression for $\mathrm{Prob}\left(\left\{\frac{C}{I} > y | \varepsilon\right\}\right)$, and thus, K_ε can be obtained.

$$\begin{aligned} &\mathrm{Prob}\left(\left\{\frac{C}{I} > y\right\}\right) \\ &\overset{(a)}{=} \int_{x=0}^{y^{-1}} \int_{\omega=-\infty}^{\infty} \Phi_{\left(\frac{C}{I}\right)^{-1}}(\omega) \, \mathrm{e}^{-j\omega x} \frac{d\omega}{2\pi} dx \\ &\overset{(b)}{=} \int_{\omega=-\infty}^{\infty} \Phi_{\left(\frac{C}{I}\right)^{-1}}(\omega) \left(\int_{x=0}^{y^{-1}} \mathrm{e}^{-j\omega x} dx \right) \frac{d\omega}{2\pi} \quad (9) \\ &\overset{(c)}{=} \begin{cases} 1, & \text{if } y \leq 0 \\ \int_{\omega=-\infty}^{\infty} \Phi_{\left(\frac{C}{I}\right)^{-1}}(\omega) \left(\frac{1 - \mathrm{e}^{-j\omega y^{-1}}}{j\omega} \right) \frac{d\omega}{2\pi}, & \text{if } y > 0, \end{cases} \end{aligned}$$

where (a) is obtained by writing the p.d.f. of $\left(\frac{C}{I}\right)^{-1}$ in terms of its characteristic function, (b) is obtained by

978-1-4244-4148-8/09/$25.00 ©2009
This full text paper was peer reviewed at the direction of IEEE Communications Society subject matter experts for publication in the IEEE "GLOBECOM" 2009 proceedings.

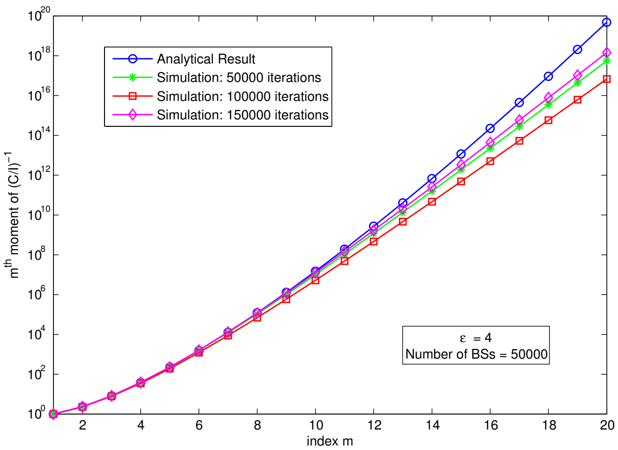

Figure 1. Comparison of m^{th} moments of $\left(\frac{C}{I}\right)^{-1}$ obtained analytically with those obtained through simulations.

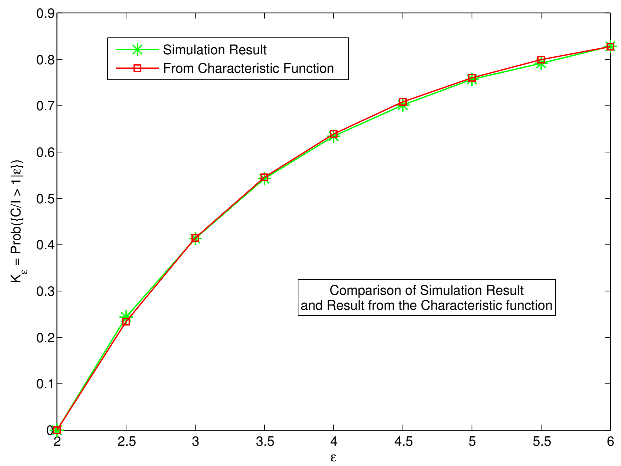

Figure 2. Comparison of the $K_\varepsilon = \text{Prob}\left(\left\{\frac{C}{I} > 1 \middle| \varepsilon\right\}\right)$ obtained through Monte-Carlo simulations with that obtained from the semi-analytical expression for various path loss exponent values.

interchanging the order of integrations, and (c) summarizes $\text{Prob}\left(\left\{\frac{C}{I} > y\right\}\right)$ for all values of y. Note that, in the expression for the tail probability of $\frac{C}{I}$ shown in (9), only the last step requires a numerical integration. From (9),

$$K_\varepsilon = \int_{\omega=-\infty}^{\infty} \Phi_{\left(\frac{C}{I}\right)^{-1}}(\omega) \left(\frac{1 - \mathrm{e}^{-j\omega}}{j\omega}\right) \frac{d\omega}{2\pi}. \quad (10)$$

Figure 2 shows the plot of K_ε vs ε comparing the semi-analytical expression with the Monte-Carlo simulations. This shows that this work is consistent with the previous attempts (cf. Fig. 4 of [2]) and precludes the need for a purely numerical approach. The performance of the SCS without shadow fading is now completely characterized.

IV. SCS Performance with Shadow Fading

In this section, the SCS is analyzed when the shadow fading is introduced. For such a system, the expression for $\frac{C}{I}$ is given in (2). This is because the MS chooses the BS corresponding to the strongest received power as the signal-carrying BS, and the signal-carrying BS need not necessarily be the closest BS. Theorem 2 analytically shows that the effect of the introduction of shadow fading to the SCS is completely captured in the average BS density. Also, it establishes the invariance of the performance, i.e. the $\frac{C}{I}$ metric, of the SCS to the shadow fading.

Theorem 2: When shadow fading in the form of independent and identically distributed (i.i.d) non-negative random factors, $\{\Psi_i\}$, is introduced to the SCS with an average BS density λ, in such a way that the Ψ_i's are independent of the random BS placement in the SCS, the resulting system is equivalent to another SCS with a different constant BS density $\bar{\lambda}$, where $\bar{\lambda} = \lambda E_\Psi\left[\Psi^{\frac{2}{\varepsilon}}\right]$, $E_\Psi[\cdot]$ is the expectation operator w.r.t the random variable Ψ, and where $f_\Psi(\cdot)$ is the p.d.f. of Ψ. Such an equivalence is valid as long as $\int_{\psi=0}^{\infty} \psi^{\frac{2}{\varepsilon}} f_\Psi(\psi)\, d\psi < \infty$.

Proof: The expression for $\frac{C}{I}$ may equivalently be written as $\frac{C}{I} = \frac{\bar{R}_1^{-\varepsilon}}{\sum_{i>1} \bar{R}_i^{-\varepsilon}}$, where $\bar{R}_1 = R_S \Psi_S^{-\frac{1}{\varepsilon}}$ and $\bar{R}_i \equiv R_i \Psi_i^{-\frac{1}{\varepsilon}}$. Recall that the subscript 'S' is used to refer to the signal-carrying BS, the subscript '1' is used to refer to the BS closest to the MS, and the subscript 'i' is used to index the interfering BSs. This expression is similar to the $\frac{C}{I}$ expression for the SCS (see Equation (1)), with the $\bar{R}$'s replacing the R's. For the rest of the proof, let R be the the random variable representing the radial distance from the MS to a base station. Then, recall from the Poisson point process, that the probability that there is one BS in $R \in (r, r + \Delta r)$ is given by $\lambda 2\pi r \Delta r + o(\Delta r)$. Let this probability measure be denoted by $P(1; r, r + \Delta r)$. Similarly, $P(0; r, r + \Delta r) = 1 - \lambda 2\pi r \Delta r + o(\Delta r)$. For the SCS, this is the probability that there is a BS in the ring of radius r and thickness Δr. Note that there can be either one or no BSs in this ring and the probability that there exists more than one BS is negligible. Such a construction has already been described in the proof of Theorem 1. Now, let $\bar{R} = R\Psi^{-\frac{1}{\varepsilon}}$, where R is as defined before, Ψ is the shadow fading factor corresponding to the BS in the ring, and $\bar{R}$ is the corresponding equivalent radial distance. Here, it is shown that $\bar{R}$ follows the same type of distribution as R, and hence, $\bar{R}$ can be viewed as a radial distance corresponding to some point in a new SCS with a new average BS density. The probability $\bar{P}(1; x, x + \Delta x)$ that there is a base station such that $\bar{R} \in (x, x + \Delta x)$ is

$$\begin{aligned}
&\bar{P}(1; x, x + \Delta x) \\
&\stackrel{(a)}{=} \text{Prob}\left(\left\{1 \text{ BS in } \bar{R} = R\Psi^{-\frac{1}{\varepsilon}} \in (x, x + \Delta x)\right\}\right) \\
&\stackrel{(b)}{=} E_\Psi\left[\text{Prob}\left(\left\{1 \text{ BS in } R \in \left(x\Psi^{\frac{1}{\varepsilon}}, (x + \Delta x)\Psi^{\frac{1}{\varepsilon}}\right)\right\}\right)\right] \\
&\stackrel{(c)}{=} E_\Psi\left[\lambda 2\pi x \Delta x \Psi^{\frac{2}{\varepsilon}} + o\left(\Delta x \Psi^{\frac{1}{\varepsilon}}\right)\right] \\
&\stackrel{(d)}{=} \lambda 2\pi E_\Psi\left[\Psi^{\frac{2}{\varepsilon}}\right] \Delta x + o(\Delta x), \quad (11)
\end{aligned}$$

where (a) follows from the definition, (b) is obtained by rewriting the event in terms of every realization of Ψ, (c) follows from the definition of R, (d) follows as long as $E_\Psi\left[\Psi^{\frac{1}{\varepsilon}} \lambda\left(x\Psi^{\frac{1}{\varepsilon}}\right)\right] < \infty$ and the condition

$\lim_{\Delta x \to 0} E_\Psi \left[\frac{o\left(\Delta x \Psi^{\frac{1}{\varepsilon}}\right)}{\Delta x} \right] = E_\Psi \left[\lim_{\Delta x \to 0} \frac{o\left(\Delta x \Psi^{\frac{1}{\varepsilon}}\right)}{\Delta x} \right]$ holds. In a similar fashion, it can be shown that $\bar{P}\left(0; x, x+\Delta x\right) = 1 - \lambda 2\pi E_\Psi \left[\Psi^{\frac{2}{\varepsilon}}\right] \Delta x + o\left(\Delta x\right)$, under the same conditions as mentioned above. It can also be shown that the random variables representing the number of BSs in two non-overlapping intervals are independent of each other. Hence, $\bar{R}$ follows a 2-D Poisson point process with an average BS density $\bar{\lambda}$.

It is clear that the equivalent system is a SCS with an average BS density $\bar{\lambda}$. Remarkably, the effective density $\bar{\lambda}$ is a constant dependent on the shadow fading distribution, as long as $\int_{u=0}^{\infty} u^{\frac{2}{\varepsilon}} f_\Psi(u) du$ converges. Note that this result holds true for a large class of distributions for the shadow fading factor Ψ, which satisfy the convergence formula shown above. ∎

Now, a specific distribution for the shadow fading is considered to demonstrate the use of Theorem 2. Recall that the shadow fading is well modeled by a log-normal distribution. So, consider $\{\Psi_i\}$ to be a sequence of i.i.d $\mathrm{Log-N}(0, \sigma^2)$ random variables. Using Theorem 2, the equivalent system is a SCS with an average BS density $\bar{\lambda} = \lambda \exp\left(\frac{2\sigma^2}{\varepsilon^2}\right)$. Since the exponential function is always greater than one, it follows that the effective average BS density in the equivalent SCS is at least as high as the average BS density of the SCS to which log-normal shadow fading is introduced, i.e., the BSs in the equivalent SCS are closer to each other compared to the original system.

As a result of Theorem 2, any system resulting from the introduction of shadow fading to the SCS may be viewed as another SCS with a different average BS density. Theorem 1 gives an expression for the tail probability of $\frac{C}{I}$ metric and also shows that the metric is independent of the average BS density. Combining these two results, it is inferred that the distribution of $\frac{C}{I}$ is invariant to shadow fading effects. Thus, the performance of the SCS remains the same even in the presence of shadow fading.

V. SCS with Power Control and Random Antennas

In this section, some variants of the power control features generally incorporated in practical cellular systems are considered and their effect on the performance of the SCS is analyzed. In the SCS, all BSs are assumed to be identical in terms of transmission powers, antenna gains, etc. In practical cellular systems, the signal-carrying BS generally has a transmission power different from the interfering BSs. This difference follows from two factors. First, the interfering BSs are communicating with MSs in their vicinity and controlling the transmitted power based on the relative locations of these MSs. Second, in schemes such as CDMA the signal-carrying BS transmits a desired signal and orthogonal to other signals. The interfering BSs are sending the so-called pseudo orthogonal signals. The result is that the signal and interfering BS powers differ by a systematic factor.

Let the systematic factor be a parameter α. Hence, the received signal power at the MS is $P_S = \alpha K R_S^{-\varepsilon}$ and the interference is $P_I = \sum_i K R_i^{-\varepsilon}$, where $\{R_i\}$ is the set of distances between the MS and the interfering BSs. Thus, the performance metric of the SCS with such a variation is given in (3). For this system, the tail probability is equal to $\mathrm{Prob}\left(\left\{\frac{C}{I} > \frac{y}{\alpha}\right\} \middle| \varepsilon\right)$ of the SCS. Note that when shadow fading is introduced to this system, the tail probability is still the same. This inference is made based on Theorem 2 and relies on the fact that the distribution of the shadow fading factor satisfies the constraint mentioned in the theorem.

Further, in case of a CDMA cellular system with perfect power control, the systematic factor, α, is not just a constant (as in the previous case), but is a function of the $\frac{C}{I}$. A perfect power control feature ensures constant $\frac{C}{I}$ performance at the MS, at all times. Using the SCS, such a situation is modeled by making $\alpha = y\left(\frac{C}{I}\right)^{-1}$, where y is the constant performance seen by the MS. The result in Theorem 1 can be used to characterize α completely, when the α's of all the BSs are modeled as independent random factors.

Now, consider a second variation where the BS powers and the antenna gains vary as a random process. Let the transmission powers and the antenna gains between BSs be uncorrelated. This can be captured by making the factor K of each of the BS random. Consider such a power control feature along with the shadow fading is introduced to the SCS with an average BS density, λ. Then, the received power at the MS is given by $P = \frac{\bar{\Psi}}{R^\varepsilon}$, where $\bar{\Psi} = K\Psi$ is a random variable. Here, Theorem 2 directly applies, and one can conclude that the distribution of $\frac{C}{I}$ of such a system is invariant to the distribution of $\bar{\Psi}$, as long as $\int_{u=0}^{\infty} u^{\frac{2}{\varepsilon}} f_{\bar{\Psi}}\left(u\right) du < \infty$ where $f_{\bar{\Psi}}(\cdot)$ is the p.d.f of $\bar{\Psi}$. For example, when $\{K_i\}$ and $\{\Psi_i\}$ are i.i.d log-normal random variables with mean 0 and variances σ_K^2 and σ_Ψ^2 respectively and independent of each other, then $\left\{\bar{\Psi}\right\}$ is a sequence of i.i.d Log-N $\left(0, \sigma_K^2 + \sigma_\Psi^2\right)$ random variables, and therefore, from Theorem 2, such a system is equivalent to the SCS with an average BS density $\bar{\lambda} = \lambda \exp\left(\frac{2\left(\sigma_K^2+\sigma_\Psi^2\right)}{\varepsilon^2}\right)$. From Section III, the performance of such a system is also completely characterized.

Consider instead the case when an ideal sectorized antenna is used with gain G and beamwidth θ. Let this antenna be randomly oriented so that a BS faces the MS with probability $\frac{\theta}{2\pi}$ in which case $K = G$. Otherwise $K = 0$. In this case, from Theorem 2, $\bar{\lambda} = \lambda G^{\frac{2}{\varepsilon}} \frac{\theta}{2\pi}$.

Note that, with the results obtained for the SCS in Section III and Section IV, it has been possible to completely characterize the performance of more and more complex systems as shown above.

VI. SCS with Multiple CGs

Wirelees LAN BSs (also known as access points) based on the IEEE802.11 standard are often assigned one of three channels. Cellular systems often use more than one channel. The impact of introducing multiple CGs to the SCS is presented here. Let N denote the number of CGs indexed $k = 1, 2, \cdots, N$. Also, let the BSs be assigned a CG randomly, where p_k is the probability that the k^{th} CG is assigned to the BS. A SCS having an average BS density λ, with such a random CG assignment strategy is equivalent to N independent SCSs with average BS densities $p_1\lambda,\ p_2\lambda,\ \cdots,\ p_N\lambda$ respectively [2]. Hence,

978-1-4244-4148-8/09/$25.00 ©2009
This full text paper was peer reviewed at the direction of IEEE Communications Society subject matter experts for publication in the IEEE "GLOBECOM" 2009 proceedings.

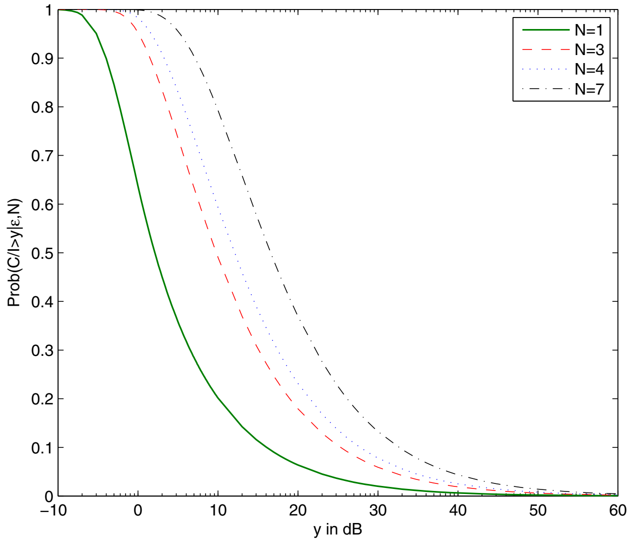

Figure 3. Comparison of $\frac{C}{I}$ performance of SCS with N CGs.

$$\text{Prob}\left(\left\{\frac{C}{I} > y \middle| \varepsilon, N\right\}\right) = 1 - \left[\text{Prob}\left(\left\{\frac{C}{I} \leq y \middle| \varepsilon\right\}\right)\right]^N .$$

In [2], an analytical expression for the above tail probability was shown for a simple case where the SCS has only two BSs. Using the results in Theorem 1, this tail probability may be obtained for any point in the support of $\frac{C}{I}$. Figure 3 shows the plot of this tail probability and illustrates the performance improvement that can be acheived by having additional CGs. Hence, the performance of the SCS with multiple CGs is also completely characterized. By combining Theorem 1 and Theorem 2, the impact on the performance of the SCS to which shadow fading is introduced along with the multiple CGs is also completely characterized. An SCS with multiple CGs models the cellular systems based on FDMA and TDMA-FDD access methods. The performance of such systems are also completely characterized using the results presented here.

VII. Simulation Methods

In this section, the details of simulating the SCS, as used for Figures 1 and 2, are presented. A single trial (or an iteration) in the experiment involves generating the SCS layout having M BSs centered at the origin, placing the MS, computing the received powers for each BS using the path loss exponent ε, and finally, computing the $\frac{C}{I}$ for the MS. Note that the distribution of $\frac{C}{I}$ is obtained by repeating the trial T times, where each trial is independent of the other. Without loss of generality, the MS is placed at the origin. For the SCS layout, the distances of the first M nearest BSs are generated using the p.d.f.'s mentioned in Section II-A. Then, the recieved powers and the $\frac{C}{I}$ can be computed. The introduction of shadow fading to the SCS may be incorporated by multiplying each of the received powers with a random number generated according to $\text{Log} - \text{N}(0, \sigma_\Psi^2)$. The introduction of random transmission gains to the SCS is also incorporated into the simulation in a similar way as it is done for the shadow fading case. When multiple CGs (say N CGs) are introduced, this situation is implemented by choosing one of the N CGs for each BS uniform randomly. In general, $M = 20000$, and $T = 20000$ is for all the simulations in this paper unless specified otherwise.

.

VIII. Conclusions

In summary, the performance of an interference-limited SCS is investigated based on the $\frac{C}{I}$ metric. The analytical results shown here prove the previous conjectures made about the SCS, and help completely characterize the performance of the SCS in practical scenarios more accurately. It is also demonstrated that the performance of the SCS is independent of the shadow fading effects, for a large class of shadow fading distributions. This surprising result, was originally conjectured in [2]. The results in this paper allow the consideration of many other sources of heterogeneities into the SCS, making the system more complicated, and still characterize their performances accurately. For example, the distribution of the $\frac{C}{I}$ of the system, which is formed by introducing random shadow fading, random transmission gains of the BSs and multiple CGs all at once, into the SCS is obtainable using the results in this paper. This motivates us to introduce more constraints and variations that are typical of practical systems, into the SCS and check what the impact of such variations on the SCS say about the practical cellular systems.

In practical cellular systems, the BS density is generally larger in densely populated areas. The approximation of constant BS density is valid as long as the path loss exponent is large enough that the larger scale variations in BS density can be ignored. The effect of variable BS densities, and more quantitative conditions on the range of validity of a constant BS density aproximation, will be explored in the future. Further application of our results to particular systems such as wireless campus LANs and distributed femtocell BSs with closed subscriber sets will be pursued later, however, the system considered here models the simple femtocell scenarios when the MS is close to the home femtocell.

References

[1] T. Brown, "Analysis and coloring of a shotgun cellular system," in *Radio and Wireless Conference, 1998. RAWCON 98. 1998 IEEE*, pp. 51–54, Aug 1998.

[2] T. Brown, "Cellular performance bounds via shotgun cellular systems," *Selected Areas in Communications, IEEE Journal on*, vol. 18, pp. 2443–2455, Nov 2000.

[3] V. Chandrasekhar, J. Andrews, and A. Gatherer, "Femtocell networks: a survey," *Communications Magazine, IEEE*, vol. 46, pp. 59–67, September 2008.

[4] H. Takagi and L. Kleinrock, "Optimal transmission ranges for randomly distributed packet radio terminals," *Communications, IEEE Transactions on*, vol. 32, pp. 246–257, Mar 1984.

[5] M. Zorzi and S. Pupolin, "Outage probability in multiple access packet radio networks in the presence of fading," *Vehicular Technology, IEEE Transactions on*, vol. 43, pp. 604–610, Aug 1994.

[6] D. Cox, "Universal digital portable radio communications," *Proceedings of the IEEE*, vol. 75, pp. 436–477, April 1987.

[7] T. S. Rappaport, *Wireless Communications: Principles and Practice*. Upper Saddle River, NJ, USA: Prentice-Hall, Inc., 1996.